Bonding in Tris(η^5-cyclopentadienyl) Actinide Complexes. 5. A Comparison of the Bonding in Np, Pu, and Transplutonium Compounds with That in Lanthanide Compounds and a Transition-Metal Analogue[1]

Richard J. Strittmatter and Bruce E. Bursten*

Contribution from the Department of Chemistry, The Ohio State University, Columbus, Ohio 43210. *Received May 21, 1990*

Abstract: Cp_3An (An = U, Np, Pu, Am, Cm, Bk, Cf) compounds have been investigated via Xα-SW molecular orbital calculations with quasi-relativistic corrections. The 5f-orbital energy drops across the series while the 6d-orbital energy rises. Due to the greater radial extension of the 6d orbitals, the metal 6d orbitals are more important in bonding the Cp ligands than the 5f orbitals. Comparison of the actinide compounds with the lanthanide series reveals some minor differences. The 4f orbitals and 6s orbital of the lanthanides are not as effective at bonding the Cp ligands as the 5f orbitals and 7s orbital of the actinides. Also, the "semicore" 5p orbitals of the lanthanides have a greater antibonding influence on the Cp ligands than do the 6p orbitals of the actinides. Comparison of the actinide compounds with $(\eta^5\text{-Cp})_3Zr$ shows some major differences. The 4d orbitals of zirconium are much more effective at bonding the Cp ligands than the 6d orbitals of the actinides.

Introduction

The 50th anniversary of the 1940 discovery of transuranium elements[2] has sparked a reinterest in the history and chemistry of these elements.[3] Although the nuclear chemistry of the transuranium elements has been thoroughly investigated, their reaction chemistry has received rather scant attention, owing, of course, to the scarcity of the elements and the difficulties in handling them. For example, in contrast to the rich organometallic chemistry developed for thorium and uranium, which are relatively abundant and easily handled, the organometallic chemistry of neptunium, plutonium, and the transplutonium elements has remained largely undeveloped.[4] In fact, only six well-documented examples of transplutonium organometallic compounds have been reported.[5-9] The few compounds known that contain a bond between carbon and a transuranium element contain either the monoanion of cyclopentadiene, $C_5H_5^-$ (Cp), or the dianion of cyclooctatetraene, $C_8H_8^{2-}$ (COT). Compounds in the latter category have been the subject of far more experimental[10] and theoretical[11] scrutiny than those in the former, which will be the focus of this contribution.

The elements Np through Cf all form Cp_3An complexes in which the trivalent actinide ion is surrounded by three Cp ligands; for two of the elements (Cm and Cf), Cp_3An is currently the only well-characterized example of an organometallic compound containing that element. The transuranium Cp_3An compounds were first prepared in the late 1960s and early 1970s. The trivalent neptunium compound was synthesized by the reduction of tetravalent Cp_3NpCl in tetrahydrofuran to give $Cp_3Np{\cdot}3THF$.[12] The plutonium[13] and transplutonium analogues were prepared by the reaction of molten bis(cyclopentadienyl)beryllium with the corresponding metal chloride, followed by fractional sublimation. These compounds were identified primarily by comparison of their infrared spectroscopy (Pu and Am) or their X-ray powder diffraction patterns (Cm, Bk, and Cf) with those of the previously synthesized Cp_3Ln (Ln = lanthanide element) compounds.

With the exception of the initial synthetic reports, few studies on the chemistry or spectroscopy of transuranium Cp_3An compounds have been reported, and all of these have been primarily concerned with the nature of the metal–Cp bonding. For example, using ^{237}Np Mössbauer spectroscopy, Karraker and Stone concluded that there is little covalency in the Np^{3+}–Cp bonding.[12] Based on infrared spectroscopy, the initial report by E. O. Fischer and co-workers on Cp_3Pu stated that the linkage between the metal and the cyclopentadienyl ligands has strong ionic character.[13] Pappalardo and co-workers performed absorption studies in which they compared the spectrum of Cp_3Am with that of americium(III) halides.[14] They concluded that the bathochromic shift of the Cp_3Am compound with respect to AmX_3 compounds is in line with the increased covalency of the organometallic compound. Finally, in an elaborate study of the absorption spectra of Cp_3Am and Cp_3Cm, Laubereau and co-workers estimated the percent f-electron covalency in these compounds.[15] They concluded that the actinide compounds are slightly more covalent than the corresponding lanthanide compounds, but are considerably less covalent than typical transition-metal cyclopentadienyls. Thus, one can see that the literature paints an extremely vague picture of the bonding in these compounds, the general theme being a very qualitative one: The An–Cp bonding has strong ionic characteristics.[16]

(1) Part 4. Bursten, B. E.; Rhodes, L. F.; Strittmatter, R. J. *J. Less-Common Met.* **1989**, *149*, 207-211.
(2) (a) McMillan, E.; Adelson, P. H. *Phys. Rev.* **1940**, *57*, 1185-1186. (b) Seaborg, G. T. *Man-Made Transuranium Elements*; Prentice-Hall: Englewood Cliffs, NJ, 1963.
(3) Recent symposia: Symposium to Commemorate the 50th Anniversary of the Discovery of Transuranium Elements. 200th American Chemical Society National Meeting, Washington, DC, August 26-31, 1990. Fifty Years with Transuranium Elements. The Robert A. Welch Foundation Conference on Chemical Research XXXIV, Houston, TX, October 22-23, 1990.
(4) (a) Marks, T. J.; Streitwieser, A. In *The Chemistry of the Actinide Elements*; Katz, J. J., Morss, L. R., Seaborg, G. T., Eds.; Chapman and Hall: New York, 1986. (b) Marks, T. J. In *The Chemistry of the Actinide Elements*; Katz, J. J., Morss, L. R., Seaborg, G. T., Eds.; Chapman and Hall: New York, 1986. (c) Marks, T. J.; Ernst, R. D. In *Comprehensive Organometallic Chemistry*; Wilkinson, G., Stone, F. G. A., Abel, E. W., Eds.; Pergamon Press: Oxford, England, 1982.
(5) Cp_3Am: Baumgärtner, F.; Fischer, E. O.; Kanellakopulos, B.; Laubereau, P. *Angew. Chem., Int. Ed. Engl.* **1966**, *5*, 134-135.
(6) $KAm(COT)_2$: Karraker, D. G. *J. Inorg. Chem. Nucl. Chem.* **1977**, *39*, 87-89.
(7) Cp_3Cm: (a) Laubereau, P. G.; Burns, J. H. *Inorg. Nucl. Chem. Lett.* **1970**, *6*, 59-63. (b) Baumgärtner, F.; Fischer, E. O.; Billich, H.; Dornberger, E.; Kanellakopulos, B.; Roth, W.; Stieglitz, L. *J. Organomet. Chem.* **1970**, *22*, C17-C18.
(8) $[Cp_2BkCl]_2$: Laubereau, P. G. *Inorg. Nucl. Chem. Lett.* **1970**, *6*, 611-616.
(9) Cp_3Bk and Cp_3Cf: Laubereau, P. G.; Burns, J. H. *Inorg. Chem.* **1970**, *9*, 1091-1095.
(10) Brennan, J. G.; Green, J. C.; Redfern, C. M. *J. Am. Chem. Soc.* **1989**, *111*, 2373-2377, and references therein.
(11) Chang, A. H. H.; Pitzer, R. M. *J. Am. Chem. Soc.* **1989**, *111*, 2500-2507, and references therein.
(12) Karraker, D. G.; Stone, J. A. *Inorg. Chem.* **1972**, *11*, 1742-1746.
(13) Baumgärtner, F.; Fischer, E. O.; Kanellakopulos, B.; Laubereau, P. *Angew. Chem., Int. Ed. Engl.* **1965**, *4*, 878.
(14) Pappalardo, R.; Carnall, W. T.; Fields, P. R. *J. Chem. Phys.* **1969**, *51*, 842-843.
(15) Nugent, L. J.; Laubereau, P. G.; Werner, G. K.; Vander Sluis, K. L. *J. Organomet. Chem.* **1971**, *27*, 365-372.
(16) Burns, C. J.; Bursten, B. E. *Comments Inorg. Chem.* **1989**, *2*, 61-93.

0002-7863/91/1513-552$02.50/0

The transuranium Cp_3An complexes, in concert with the extensive chemistry of Cp_3Th and Cp_3U, provide a potentially rich area for the study of molecular bonding in a homologous series of complexes spanning the early to late actinide elements. Although the bonding trends in these compounds are exceedingly difficult to study experimentally, theoretical studies are quite tractable. Therefore, as an extension fo our theoretical studies on organoactinide compounds,[17] we have undertaken Xα-SW molecular orbital calculations with quasi-relativistic effects on the series Cp_3An where An = U, Np, Pu, Am, Cm, Bk, and Cf. This series allows us to compare the actinides within a common, yet realistic, molecular framework. We will first consider a general bonding picture for the entire series with emphasis on the role of the 5f vs 6d orbitals in bonding as a function of metal. To accomplish this we will need to look at the relative energetics and the radial extensions of these orbitals. Then, in an attempt to address the question of the nature of the metal–carbon bonds in these compounds, we will compare these results with those we have obtained for the analogous Cp_3Ln compounds and for a transition-metal analogue.

Assumed Structures of Cp_3An Compounds

Chemists have been curious about the structure of Cp_3An compounds since they were first synthesized. To date, no structures have been fully resolved for the actinide compounds with unsubstituted Cp ligands, although two structures have been reported with modified Cp ligands: $Cp^{\ddagger}_3Th$ [$Cp^{\ddagger} = \eta^5$-$C_5H_3(SiMe_3)_2$][18] and $Cp^{\dagger}_3U$ [$Cp^{\dagger} = \eta^5$-$C_5H_4(SiMe_3)$].[19] Both of these compounds consist of discrete molecules that exhibit a pseudo-D_{3h} structure in which the metal and the three Cp centroids all lie in one plane with Cp(centroid)–M–Cp(centroid) angles of approximately 120°. X-ray powder diffraction data for Cp_3Cm, Cp_3Bk, and Cp_3Cf[7a,9] have established that the crystal structures of these actinide compounds are isomorphous with the analogous Cp_3Ln compounds where Ln = Pr, Pm, Sm, Gd, and Tb. Recently, R. D. Fischer and co-workers resolved the structures of several Cp_3Ln compounds.[20] They determined that Cp_3Pr is a polymeric compound consisting of zig-zag chains of distinct $(\eta^5\text{-Cp})_2\text{Pr}(\mu\text{-}\eta^2,\eta^5\text{-Cp})$ units.[21]

Although it seems likely that the later actinide compounds are of the polymeric form found for Cp_3Pr, we have chosen to investigate these compounds in the pseudo-D_{3h} geometry for several reasons: (1) The D_{3h} geometry presents an obvious and logical comparison to Cp_3An compounds of the early actinides. (2) These structures may be treated as discrete molecules. (3) The higher symmetry of this geometry makes these large calculations feasible and facilitates interpretation of the results.

A judicious choice for the An–C distance in these compounds is also a consideration. The An–C distances of $Cp^{\ddagger}_3Th$ and $Cp^{\dagger}_3U$ are 2.80[18] and 2.78 Å,[19] respectively. The U–C(Cp) distance has also been determined for several U(III) Cp_3UL compounds. These distances generally fall in the range of 2.76–2.82 Å.[22] As mentioned above, no crystal structures of transuranium Cp_3An compounds or their derivatives have been reported. However, structures have been determined for Cp_3Ln compounds[20,21,23] and their derivatives[24] throughout the lanthanide series. In general, the change in the Ln–C(Cp) distances mirrors the change in the +3 ionic radii of the metals in these compounds. We have therefore chosen to study the Cp_3An compounds at two different An–C distances. In the first set of calculations, a constant An–C distance of 2.79 Å was used for the entire series. In the second, the An–C distance was varied consistently across the series Cp_3Np (2.77 Å), Cp_3Pu (2.76 Å), Cp_3Am (2.74 Å), Cp_3Cm (2.73 Å), Cp_3Bk (2.72 Å), and Cp_3Cf (2.70 Å). These choices reflect the differences of ionic radii for these An(III) metals from that of U(III).[25] Unless noted otherwise, the values reported here are for the latter An–C distances.

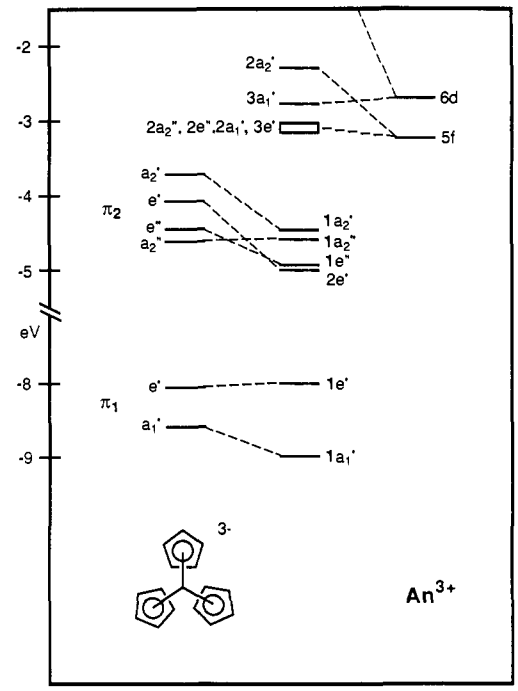

Figure 1. Molecular orbital diagram depicting the interaction of the Cp_3^{3-} ligand field with a typical actinide metal. The actinide atomic orbital energies are approximate. Due to large intersphere contributions, the energy of the 7s orbital is not plotted.

Table I. Metal Orbital Interactions with Cp_3^{3-} under D_{3h} Symmetry

D_{3h} rep	Cp_3^{3-} orbital	metal orbitals
a_1'	π_1	s; $d_{z^2}(d\sigma)$; $f_{x(x^2-3y^2)}(f\phi)$
a_2'	π_2	$f_{y(3x^2-y^2)}$ $(f\phi)$
e'	π_1, π_2	p_x,p_y $(p\pi)$; $d_{x^2-y^2}$, d_{xy} $(d\delta)$; f_{xz^2}, f_{yz^2} $(f\pi)$
a_1''	none	none
a_2''	π_2	p_z $(p\sigma)$; f_{z^3} $(f\sigma)$
e''	π_2	d_{xz},d_{yz} $(d\pi)$; $f_{xyz},f_{z(x^2-y^2)}$ $(f\delta)$

Results and Discussion

In a previous account, we discussed in detail the interactions between uranium and three Cp ligands under C_{3v} symmetry.[17a] We will therefore give only a brief background of the general bonding considerations and then concentrate on the interactions that are crucial to the arguments here. Although the current calculations were performed under C_{3v} symmetry, the metal–Cp bonding shows little deviation from virtual D_{3h} symmetry. We will therefore discuss the bonding in Cp_3An compounds in terms of D_{3h} symmetry.

(17) (a) Bursten, B. E.; Rhodes, L. F.; Strittmatter, R. J. *J. Am. Chem. Soc.* **1989**, *111*, 2758–2766. (b) Bursten, B. E.; Rhodes, L. F.; Strittmatter, R. J. *J. Am. Chem. Soc.* **1989**, *111*, 2756–2758. (c) Bursten, B. E.; Strittmatter, R. J. *J. Am. Chem. Soc.* **1987**, *109*, 6606–6608.

(18) Blake, P. C.; Lappert, M. F.; Atwood, J. L.; Zhang, H. *J. Chem. Soc., Chem. Commun.* **1986**, 1148–1149.

(19) (a) Brennan, J. G. Ph.D. Dissertation, University of California, Berkeley, 1985. (b) Zalkin, A.; Brennan, J. G.; Andersen, R. A. *Acta Crystallogr., Sect. C: Cryst. Struct. Commun.* **1988**, *C44*, 2104.

(20) (a) Eggers, S. H.; Hinrichs, W.; Kopf, J.; Jahn, W.; Fischer, R. D. *J. Organomet. Chem.* **1986**, *311*, 313–323. (b) Eggers, S. H.; Schultze, H.; Kopf, J.; Fischer, R. D. *Angew. Chem., Int. Ed. Engl.* **1986**, *25*, 656–657. (c) Eggers, S. H.; Kopf, J.; Fischer, R. D. *Organometallics* **1986**, *5*, 383–385.

(21) Hinrichs, W.; Melzer, D.; Rehwoldt, M.; Jahn, W.; Fischer, R. D. *J. Organomet. Chem.* **1983**, *251*, 299–305.

(22) (a) Wasserman, H. J.; Zozulin, A. J.; Moody, D. C.; Ryan, R. R.; Salazar, K. V. *J. Organomet. Chem.* **1983**, *254*, 305–311. (b) Brennan, J. G.; Andersen, R. A.; Zalkin, A. *Inorg. Chem.* **1986**, *25*, 1761–1765. (c) Brennan, J. G.; Stults, S. D.; Andersen, R. A.; Zalkin, A. *Organometallics* **1988**, *7*, 1329–1334.

(23) (a) Rebizant, J.; Apostolidis, C.; Spirlet, M. R.; Kanellakopulos, B. *Acta Crystallogr.* **1988**, *C44*, 614–616. (b) Burns, J. H.; Baldwin, W. H.; Fink, F. H. *Inorg. Chem.* **1974**, *13*, 1916–1920. (c) Wong, C.-H.; Lee, T.-Y.; Lee, Y.-T. *Acta Crystallogr.* **1969**, *B25*, 2580–2587.

(24) (a) Rogers, R. D.; Vann Bynum, R.; Atwood, J. L. *J. Organomet. Chem.* **1980**, *192*, 65. (b) Baker, E. C.; Raymond, K. N. *Inorg. Chem.* **1977**, *16*, 2710–2714. (c) Burns, J. H.; Baldwin, W. H. *J. Organomet. Chem.* **1976**, *120*, 361–368.

(25) Bagnall, K. W. *The Actinide Elements*; Elsevier: Amsterdam, 1972; Chapter 2.

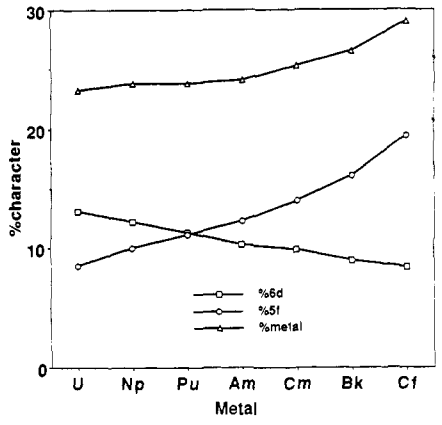

Figure 2. Graph of the total metal participation in the π_2-based molecular orbitals for the compounds Cp_3U through Cp_3Cf and its breakdown into the amount of 5f- and 6d-orbital participation.

The primary metal–Cp bonding interactions take place between the valence orbitals of the actinide metal and the highest occupied degenerate set of e_1'' (π_2) orbitals on the D_{5h} Cp ligands. A secondary bonding interaction occurs between the metal valence orbitals and the next highest a_2'' π orbital of the Cp ligands, the π_1 orbital. As demonstrated in our previous studies, when three Cp ligands are placed about a central point under 3-fold symmetry at a typical An–Cp distance, the Cp π_2 orbitals are strongly split by ligand–ligand interactions. Under D_{3h} symmetry, these orbitals transform as $a_2' + e' + a_2'' + e''$, while the π_1 orbitals transform as $a_1' + e'$. A molecular orbital diagram depicting the interaction of the Cp_3^{3-} ligand field with an An^{3+} ion for a typical Cp_3An compound is pictured in Figure 1. Table I lists the possible interactions of the metal orbitals with the Cp_3^{3-} orbitals under D_{3h} symmetry. Using this high symmetry, we will be able to focus on certain interactions to elucidate the bonding in these compounds.

As a first approximation, we will consider the total actinide atom participation in the An–Cp π_2-bonding orbitals (the 2e', 1e'', $1a_2''$, and $1a_2'$ orbitals), which is plotted as a function of metal in Figure 2. Also plotted is the breakdown of this total metal participation into 5f and 6d atomic orbital contributions. The sum of the 5f-orbital and 6d-orbital contributions is approximately equal to the total metal participation. Therefore, the metal 5f and 6d orbitals are primarily responsible for bonding the Cp ligands, i.e., the valence 7s and 7p orbitals play a negligible role in the Cp π_2 orbitals. Considering only the total metal participation in the An–Cp π_2 bonding orbitals, it appears that the metal–ligand interaction in these compounds increases to the right of the series. This is far from the whole picture, for we must consider the origin of these effects.

While details of the Xα–SW method have been described elsewhere,[26] we point out here that one of the major disadvantages of the method is the numerical, as opposed to analytical, nature of the orbitals.[27] This is in contrast to conventional LCAO–MO methods wherein population analysis of eigenvectors is generally used to facilitate interpretation. It is possible to partition an Xα–SW orbital into its contributions from the various atomic spheres (as was done to obtain the results in Figure 2), but this analysis does not indicate the bonding, nonbonding, or antibonding character of the orbital, nor does it indicate the degree of interaction between the atoms. In order to extract this information from the calculations, we must consider the stabilization (or destabilization) of certain molecular orbitals. In general, the greater the stabilization (or destabilization) of certain metal atomic orbitals or ligand-based fragment orbitals, the greater the interaction between the metal and the ligands.[28]

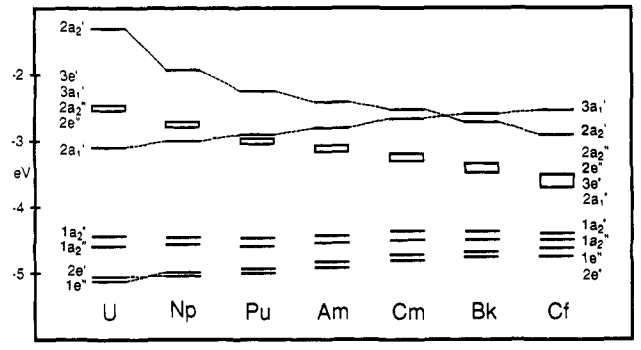

Figure 3. Molecular orbital diagram of the π_2-based molecular orbitals and the metal-based molecular orbitals for the compounds Cp_3U through Cp_3Cf. The $2a_1'$ orbital of Cp_3U is the s/d_{z^2} hybrid orbital (see text).

Table II. Energies (eV) of Selected Molecular Orbitals and $\Delta E_{f\phi}$ (eV) for Cp_3M Compounds

	orbital energies, eV			
compd	$E(d\sigma)^a$	$E(f\phi_{non})^b$	$E(f\phi_{anti})^c$	$\Delta E_{f\phi}{}^d$
Cp_3U	-3.10	-2.46	-1.61	0.85
Cp_3Np	-2.98	-2.76	-1.91	0.85
Cp_3Pu	-2.89	-2.98	-2.15	0.83
Cp_3Am	-2.77	-3.13	-2.31	0.82
Cp_3Cm	-2.66	-3.30	-2.47	0.83
Cp_3Bk	-2.57	-3.47	-2.62	0.85
Cp_3Cf	-2.52	-3.73	-2.82	0.91
Cp_3Ce	-2.87	-2.68	-2.17	0.51
Cp_3Pr	-2.78	-2.95	-2.43	0.52
Cp_3Nd	-2.71	-3.12	-2.60	0.52
Cp_3Sm	-2.59	-3.35	-2.82	0.53
Cp_3Gd	-2.49	-3.51	-2.97	0.54
Cp_3Dy	-2.42	-3.67	-3.11	0.56
Cp_3Zr	-3.92			

[a] $2a_1'$ orbital for M = U, Np, Ce, and Zr; $3a_1'$ orbital for M = Pu – Cf and Pr – Dy. [b] $3a_1'$ orbital for M = U, Np, and Ce; $2a_1'$ orbital for M = Pu – Cf and Pr – Dy. [c] $2a_2'$ orbital. [d] $\Delta E_{f\phi} = E(f\phi_{anti}) - E(f\phi_{non})$.

In order to assess stabilization (or destabilization) of orbitals, let us consider the relative energy of the 5f orbitals vs the 6d orbitals. The energies of the highest occupied and the lowest unoccupied orbitals for the entire series, Cp_3U through Cp_3Cf, are plotted in Figure 3. The relative energetic ordering of the atomic 5f and 6d orbitals of the metals can be obtained indirectly by looking at the actinide orbitals that are forbidden by symmetry from interacting with the Cp π_2 orbitals. These orbitals all transform as a_1' representations under D_{3h} symmetry (Table I). The $f_{x(x^2-3y^2)}$ orbital (one of the fϕ orbitals) is the lone f orbital that falls into this category. As such, this nonbonding orbital is a reference for the unperturbed 5f-orbital energy for a given compound. A steady drop in energy amounting to nearly 1.3 eV is observed for this orbital across the series (-2.46 eV in Cp_3U to -3.73 eV in Cp_3Cf, Table II). As has been noted previously,[17b] the d_{z^2} orbital is also forbidden by symmetry from interacting with the ligands. This orbital mixes slightly with the 7s orbital[29] so it will not be a true indication of the unperturbed 6d-orbital energy, but nevertheless, it will give an indication of the general trend of the energy of the 6d orbitals as a function of metal. This orbital shows a steady rise in energy across the series (-3.10 eV in Cp_3U to -2.52 eV in Cp_3Cf, Table II). These energetic trends across the series are consistent with experimental work on the free, triply ionized metal ions[30] and also agree with computational results for

(26) The Xα–SW method has been the subject of several review articles: (a) Slater, J. C. *Solid-State and Molecular Theory: A Scientific Biography*; Wiley: New York, 1975. (b) Johnson, K. H. *Annu. Rev. Phys. Chem.* **1975**, *26*, 39. (c) Case, D. A. *Annu. Rev. Phys. Chem.* **1982**, *33*, 151–171.

(27) The advantages and disadvantages of the Xα–SW method for organo-f-element complexes have been discussed in detail elsewhere: Bursten, B. E.; Fang, A. *Inorg. Chim. Acta* **1985**, *110*, 153–160.

(28) Albright, T. A.; Burdett, J. K.; Whangbo, M.-H. *Orbital Interactions in Chemistry*; Wiley: New York, 1985.

(29) By symmetry, all three of the a_1' orbitals (the 7s, the $6d_{z^2}$, and the $5f_{x(x^2-3y^2)}$ are allowed to mix, but in the calculational results it is found that the $5f_{x(x^2-3y^2)}$ has negligible mixing with the other two orbitals. The one exception to this is Cp_3Pu, in which the s/d_{z^2} hybrid orbital is found to have 5% $5f_{x(x^2-3y^2)}$ character.

$AnCl_3$ compounds.[1] Thus, the 6d orbitals have a more favorable energy match with the Cp π_2 orbitals to the left of the series while the 5f orbitals have a more favorable energy match to the right of the series.

Consistent with the above energetic trends, the 6d-orbital participation in the metal–ligand bonding orbitals decreases across the series while the 5f-orbital participation increases dramatically (Figure 2). This results in a situation where the 6d orbitals participate more to the left of the series while the 5f orbitals dominate on the right. We must now consider two questions: (1) Does the increase in f-orbital participation truly reflect an increase of f-orbital–Cp interaction (or, conversely, does the decrease of d-orbital participation truly reflect a decrease of d-orbital–Cp interaction)? and (2) Should the 5f orbitals and 6d orbitals be considered on an equal scale with respect to An–Cp bonding?

Turning to the An–Cp bonding orbitals, we see that the a_2' orbital is restricted by symmetry to interact with only one metal valence orbital, the remaining $f\phi$ orbital. The interligand antibonding nature of the ligand-based a_2' orbital significantly destabilizes it (Figure 1), resulting in a very favorable energy match with the 5f orbitals. In addition, the $f\phi$ orbitals lie in the plane of the Cp centroids, facilitating strong interaction with the Cp ligands.[31] Consistent with the energetic lowering of the 5f orbitals across the series, the metal participation in the $1a_2'$ orbital increases dramatically across the series (total metal participation in the $1a_2'$ orbital: 29% 5f in Cp_3U to 55% 5f in Cp_3Cf). The antibonding counterpart of this bonding interaction, the $2a_2'$ MO, is destabilized above the remaining 5f orbitals (Figure 1).[32] Inasmuch as this interaction is purely Cp π_2–metal 5f in character, the extent of destabilization of the antibonding $2a_2'$ orbital from the nonbonding 5f orbital can be used as a measure of the Cp-bonding capability of the 5f orbitals. In other words, the larger the $5f\phi$–$5f\phi$ splitting ($\Delta E_{f\phi}$, Table II), the greater the interaction between the metal 5f orbitals and the ligand-based orbitals. As can be seen in Table II, the $5f\phi$–$5f\phi$ splitting is nearly constant for the entire series, indicating that the Cp-bonding ability of the 5f orbitals is approximately equal for the entire series.

The only deviation from this generalization is Cp_3Cf, which warrants some discussion. The somewhat greater value of $\Delta E_{f\phi}$ is probably due to an almost exact computational energy match between its 5f orbitals (−3.73 eV) and the a_2' orbital of the metal-free Cp_3^{3-} ligand field (−3.65 eV).[33] This effect is not observed for the remaining eight members of the series, in spite of the fact that the differences in energy between the metal 5f orbitals and the ligand-based a_2' orbital span a wide energetic range, from 1.31 eV for Cp_3U to 0.16 eV for Cp_3Bk. It should be noted here that the fragment orbitals primarily give an indication of the stabilization (or destabilization) that a given orbital undergoes upon interaction with the second fragment, and not a true indication of the ligands as separate entities. Also, it has been noted elsewhere that one of the problems with the Xα–SW method is the large intersphere charge contributions in the ligand π-based valence orbitals, which artificially raises the energy of these molecular orbitals relative to the more localized metal-based levels.[34] This will, of course, affect the Cp π_2-based molecular orbitals, which will in turn affect the Cp π_2 fragment orbitals. Both of these factors suggest that the absolute energies of the Cp π_2 fragment orbitals should not be fully trusted. Therefore, we are not suggesting that a special situation exists that would affect the chemistry of Cp_3Cf relative to the rest of the series. Rather, the calculations show that the interaction between the 5f orbitals and the ligand-based orbitals does not increase across the series and this situation changes *only* when an extremely close energy match exists between the two.[35] Therefore, the domination of the 5f orbitals in the Cp-bonding orbitals of the later actinides (Figure 2) is primarily due to a coincidental energy match of these 5f orbitals with the Cp π_2 orbitals, which does not necessarily lead to greater metal–ligand bonding.

This lack of increased π_2–5f interaction for the later actinides, despite a more favorable energy match between the 5f orbitals and the ligand orbitals, can be explained by the contraction of the 5f orbitals across the series. As an example of this, contour diagrams of the $5f_{z^3}$ orbitals for Cp_3Np and Cp_3Cf are plotted in Figure 4. This contraction results in a poorer overlap between the metal orbitals and the ligand orbitals for the later actinide compounds.

We now turn our attention to the two orbitals in which the 5f and 6d orbitals can compete, the e′ and e″ orbitals. For the e′ orbital, the $5f\pi$ and $6d\delta$ metal orbitals can both interact with the ligand-based orbital. As was the case with the $5f\phi$ orbital discussed above, the $6d\delta$ orbitals lie in the plane of the Cp centroids directed toward the Cp π orbitals, resulting in a strong interaction. In contrast, the $5f\pi$ orbitals are directly primarily along the 3-fold axis (the z axis) and thus are not well directed toward the Cp π orbitals. This causes the e′ interaction to be dominated by the

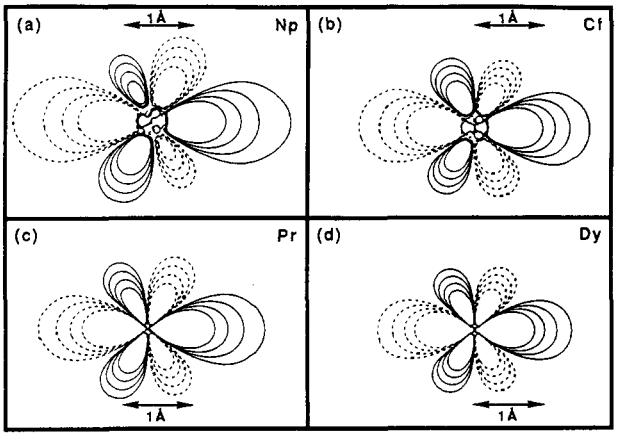

Figure 4. Contour diagrams of the $2a_2''$ orbital of (a) Cp_3Np, (b) Cp_3Cf, (c) Cp_3Pr, and (d) Cp_3Dy. The contour values are ±0.135, ±0.090, ±0.060, and ±0.040. The double-headed arrow represents 1 Å.

Table III. Stabilization Energies (eV) of Ligand-Based Orbitals upon Interaction with Different Metal Atoms[a]

	π_2				π_1	
compd	$1a_2'$	2e′	1e″	$1a_2''$	1e′	$1a_2'$
Cp_3U	0.69	0.95	0.62	−0.07	−0.01	0.33
Cp_3Np	0.74	0.95	0.57	−0.05	−0.03	0.33
Cp_3Pu	0.75	0.93	0.51	−0.05	−0.04	0.32
Cp_3Am	0.77	0.92	0.48	−0.06	−0.06	0.32
Cp_3Cm	0.81	0.92	0.44	−0.04	−0.04	0.35
Cp_3Bk	0.84	0.91	0.41	−0.01	−0.05	0.35
Cp_3Cf	0.92	0.92	0.38	0.01	−0.06	0.36
Cp_3Ce	0.54	0.87	0.54	−0.19	−0.12	−0.06
Cp_3Pr	0.56	0.87	0.49	−0.17	−0.12	−0.04
Cp_3Nd	0.58	0.86	0.46	−0.17	−0.12	−0.05
Cp_3Sm	0.61	0.88	0.40	−0.16	−0.12	−0.03
Cp_3Gd	0.63	0.90	0.36	−0.14	−0.10	0.00
Cp_3Dy	0.66	0.91	0.31	−0.11	−0.09	0.02
Cp_3Zr	0.03	1.43	0.86	−0.01	0.15	0.28

[a] The stabilization energy is defined as the energy of the ligand-based orbital in the metal complex minus the energy of the orbital in the Cp_3 ligand set.

(30) Brewer, L. *J. Opt. Soc. Am.* **1971**, *61*, 1666–1682.

(31) For a discussion of the shapes of f orbitals see: (a) Friedman, H. G.; Choppin, G. R.; Feuerbacher, D. G. *J. Chem. Educ.* **1964**, *41*, 354–358. (b) Becker, C. *J. Chem. Educ.* **1984**, *41*, 358–360. (c) Ogryzlo, E. A. *J. Chem. Educ.* **1965**, *42*, 150–151.

(32) A contour diagram of the bonding and antibonding molecular orbitals of this interaction in Cp_3U is depicted in Figure 3 of ref. 17a.

(33) The energies of the metal-free ligand-based orbitals (the fragment orbitals) cannot be obtained directly from the Xα–SW calculation. The process for obtaining these values is described in Computational Details and has been described elsewhere: (a) Braydich, M. D.; Bursten, B. E.; Chisholm, M. H.; Clark, D. L. *J. Am. Chem. Soc.* **1985**, *107*, 4459–4465. (b) Bursten, B. E.; Cotton, F. A. *Inorg. Chem.* **1981**, *20*, 3042–3048.

(34) Cotton, F. A.; Stanley, G. G.; Cowley, A. H.; Lattman, M. *Organometallics* **1988**, *7*, 835–840.

(35) A similar situation has been observed with the $An(COT)_2$ series: Boerrigter, P. M.; Baerends, E. J.; Snijders, J. G. *Chem Phys.* **1988**, *122*, 357–374.

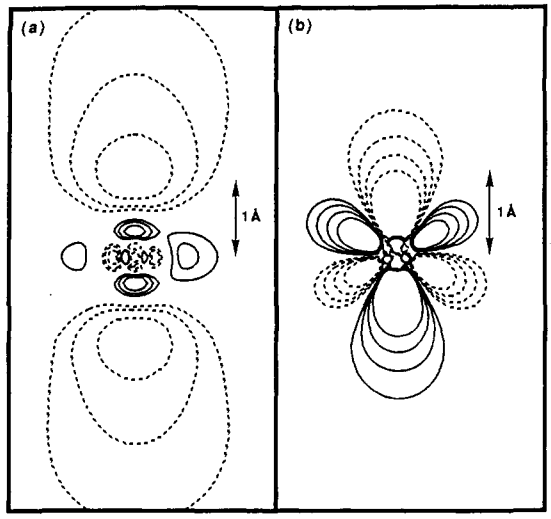

Figure 5. Contour diagrams of (a) the $3a_1'$ orbital of Cp_3Am and (b) the $2a_2''$ orbital of Cp_3Am. The contour values are ±0.135, ±0.090, ±0.060, and ±0.040. The double-headed arrow represents 1 Å.

dδ orbitals, regardless of actinide metal. In contrast to the situation observed for the $1a_2'$ orbital, the metal participation in the 2e′ orbital shows little sensitivity to the energies of the metal orbitals, decreasing only slightly across the series (total metal participation in the 2e′ orbital for Cp_3Np: 2% p, 16% 6d, 1% 5f; for Cp_3Cf: 2% p, 12% 6d, 2% 5f).[36] As measured by the stabilization of the corresponding ligand-based orbitals upon interaction with the metal atom (Table III), the 2e′ orbital interaction is approximately equal for all of the actinide metals. Also, despite the much greater metal participation in the $1a_2'$ orbital, the metal–ligand interaction is actually greatest in the 2e′ orbital (the one exception being Cp_3Cf, discussed above).

Next, the 1e″ orbital can interact both with the 5fδ and the 6dπ orbitals. We will see that this interaction is crucial to the interpretation of these results. The angular portions of these orbitals are comparable: Both sets are similarly directed toward the Cp π orbitals. This creates a situation in which the relative energies of the 5f and 6d orbitals of the metal will determine which will participate in this bonding orbital. Quantitatively, the total metal participation in the 1e″ orbital stays approximately the same for the entire series, ranging from 25% to 28%. When this total metal participation is broken down into the individual metal orbital contributions, we find that the 1e″ orbital of the early actinides is dominated by the 6dπ orbitals: Cp_3U and Cp_3Np have a 6dπ/5fδ ratio of approximately 80:20. This situation changes markedly to the right of the series, with Cp_3Bk and Cp_3Cf having a 6dπ/5fδ ratio of approximately 45:55.

Looking more closely at this orbital, we see that upon interaction with the metal, the ligand-based e″ orbital is most stabilized for the early actinides (Table III). In fact, the 1e″ orbital is lower in energy than the 2e′ orbital for Cp_3U, while for the rest of the series, the 2e′ orbital lies lower in energy (Figure 3). Thus, although the total metal participation in this orbital remains constant across the series, the extent of the metal–ligand interaction actually decreases. Inasmuch as the 5f orbitals participate to a much greater extent to the right of the series, and the metal–ligand interaction is lower in this region, we can further state that the 6d orbitals are interacting more strongly with the ligands and, hence, are more effective at accepting charge from the ligands than the 5f orbitals.

To help explain the above observations we must consider the radial extension of the 5f orbitals in comparison with the 6d orbitals. Contour plots of the 5fσ orbital and the 6dσ orbital for Cp_3Am demonstrate the dramatic size difference between the two sets of orbitals (Figure 5). It is clear that the greater radial extension of the 6d orbitals will allow them to overlap with the ligand orbitals to a much greater extent than the 5f orbitals, especially at the long An–C distances found for Cp ligands.

A few comments concerning the remaining bonding orbitals are in order. First, the $1a_2''$ and the π_1-based 1e′ orbitals, are nearly unaffected by the metal atom (Table III). For the 1e′ orbital, this can best be explained as a balance between two opposing, albeit weak, interactions. As was the case with the 2e′ orbital, the metal 6dδ orbitals interact with the ligand orbital, although to a much lesser extent due to a poorer energy match. Little, if any, bonding interaction is expected. The second interaction is that between the ligand orbital and the pπ orbitals of the metal. Although the pπ orbitals are well directed toward the Cp π orbitals, due to energy considerations this interaction is also expected to be small. If this interaction involves the filled 6p orbitals instead of the empty 7p orbitals of the actinide, then it will be a "filled–filled" interaction and will actually destabilize the fragment orbital. Situations in which the ligand orbitals preferentially interact with actinide 6p orbitals have been well documented.[37] Whether the 6p or 7p orbitals (or a balance of both) are involved in this interaction cannot be determined directly from the Xα–SW results, but the fact that the 1e′ orbitals are slightly destabilized suggests that the 6p orbitals are influencing the bonding in this orbital. Nevertheless, this orbital is not of significance in the overall bonding picture.

The $1a_2''$ orbital is also involved in a balance between two weak interactions. The metal 5fσ and pσ orbitals participate in this orbital. Both of these are directed along the 3-fold axis of the molecule, leading to a small interaction with the Cp ligands. The 5fσ participation increases from 11% to Cp_3U to 27% in Cp_3Cf while the pσ participation remains constant across the series at 4%. For the later actinides, the 5fσ orbital is slightly destabilized relative to the nonbonding 5f orbital (0.17 eV for Cp_3Cf). Despite the large participation of the metal 5fσ orbital in this molecular orbital, the bonding interaction is negligible, with the metal 6pσ orbital antibonding interaction balancing any bonding gained from the 5fσ orbital.

Finally, the π_1-based $1a_1'$ orbital interacts primarily with the actinide 7s orbital. The somewhat large energy separation between the 7s orbital and the ligand-based a_1' orbital relegates this orbital to a secondary role in the bonding, but the stabilization of the fragment orbital indicates that the interaction is nontrivial (Table III) and should be considered in the overall bonding picture. This interaction is approximately equal for the entire series.

Cp_3Ln Compounds. For obvious reasons, such as the high radioactivity of the later actinides, the chemistry of the Cp_3Ln series has been studied much more extensively than that of Cp_3An.[4c] It has been shown chemically and by magnetic moment measurements that the Ln–Cp bond is highly ionic.[38] As mentioned previously, a comparative study of Cp_3Ln and Cp_3An compounds concluded that the Cp_3Ln compounds have slightly less covalent character in the M–Cp bonds than the Cp_3An compounds, and that both series have considerably less covalent character than typical transition-metal–Cp bonds.[15]

We have investigated the Cp_3Ln compounds Cp_3Ce (M–C = 2.79 Å), Cp_3Pr (2.78 Å), Cp_3Nd (2.76 Å), Cp_3Sm (2.73 Å), Cp_3Gd (2.71 Å), and Cp_3Dy (2.69 Å). In order to compare the results directly, we have used the same geometry as for the Cp_3An compounds. Therefore, the symmetry arguments discussed above will hold here. We will analyze these results with an emphasis on the differences between the 4f and 5d orbitals of the lanthanide metals and the 5f and 6d orbitals of the actinide metals.

The total metal participation in the M–Cp π_2 bonding orbitals of the Cp_3Ln compounds follows the same general trend observed

(36) The 2e′ and 1e″ orbitals are nearly isoenergetic in Cp_3U, resulting in mixing of these orbitals, which both transform as e representations under the lower C_{3v} symmetry of the calculations. Therefore, the value for Cp_3Np is given here. In no way does this affect the arguments.

(37) (a) Tatsumi, K.; Hoffmann, R. *Inorg. Chem.* **1980**, *19*, 2656–2658. (b) Larsson, S.; Pyykkö, P. *Chem. Phys.* **1986**, *101*, 355–369.

(38) (a) Birmingham, J. M.; Wilkinson, G. *J. Am. Chem. Soc.* **1956**, *78*, 42–44. (b) Fischer, E. O.; Fischer, H. *J. Organomet. Chem.* **1965**, *3*, 181–187. (c) Calderazzo, F.; Pappalardo, R.; Losi, S. *J. Inorg. Nucl. Chem.* **1966**, *28*, 987–999. (d) Manastyrskyj, S.; Dubeck, M. *Inorg. Chem.* **1964**, *3*, 1647. (e) Tsutsui, M.; Takino, T.; Lorenz, D. *Z. Naturforsch., B* **1966**, *21*, 1–2.

for the Cp_3An series, including the relative participation of the atomic 4f orbitals and 5d orbitals. Consistent with this, the energies of the 4f orbitals and 5d orbitals also follow the same general trends as their actinide counterparts, although slight differences exist. Like the 5f orbitals, the 4f orbitals drop in energy across the series, but this drop is less pronounced for the 4f orbitals, amounting to 1.0 eV across nine lanthanide metals compared with >1.2 eV across seven actinides (Table II). The rise of the 5d-orbital energies is also slightly less pronounced than that of the 6d orbitals, amounting to <0.5 eV across nine lanthanides compared with 0.6 eV across seven actinides. It is worth noting that the orbital energies of the valence f and d orbitals of the early lanthanides resemble those of the middle actinide metals. For example, the energies of the 4f orbitals and 5d orbitals of the first lanthanide compound, Cp_3Ce, are approximately equal to the 5f-orbital energy of the compound of the fourth actinide, Cp_3Np, and the 6d-orbital energy of the compound of the fifth actinide, Cp_3Pu, respectively.

Turning to the Ln–Cp bonding orbitals, we will first consider the 2e′ and 1e″ orbitals, those in which the 6d orbitals of the actinides dominate the bonding. The 2e′ orbital of the lanthanide compounds is essentially identical with that of the actinide compounds. The metal participation in this orbital decreases only slightly across the series with the relative atomic orbital participation mirroring that of the actinides: the 2e′ MO of Cp_3Pr contains metal contributions of 2% p, 16% 5d, 1% 4f, while in Cp_3Dy the contributions are 2% p, 13% 5d, 1% 4f.[39] The stabilization of the corresponding ligand orbital is slightly less than that found for the actinide compounds, but by an amount that is probably insignificant considering the approximate nature of these values (Table III). Overall, the 5dδ orbitals of the lanthanides dominate this interaction and are as effective at accepting charge from the ligands as the 6dδ orbitals of the actinides.

The 1e″ orbital of the lanthanide compounds is also similar to its actinide counterpart, although some differences exist. The total metal participation is similar, ranging from 24% to 26% for the lanthanides, but the breakdown into valence fδ and dπ orbital participation is slightly different: Cp_3Ce and Cp_3Pr have 5dπ/4fδ ratios of approximately 85:15 while Cp_3Dy has a ratio of approximately 65:35. In other words, the 5dπ orbitals of the lanthanides participate slightly more than the 6dπ orbitals of the actinides (maximum participation: 22% 5dπ in Cp_3Pr; 20% 6dπ in Cp_3Np), while the 4fδ orbitals of the lanthanides participate less than the 5fδ orbitals of the actinides (maximum participation: 8% 4fδ in Cp_3Dy; 15% 5fδ in Cp_3Cf). The stabilization of the corresponding ligand orbital decreases across the series and is slightly less than the stabilization found in the actinide compounds.

We now turn to the orbitals showing significant differences between the lanthanides and the actinides. The most important of these is the $1a_2'$ orbital, which, as noted earlier, can interact only with the f orbitals. As with the actinides, the metal participation in this orbital increases dramatically across the series (28% 5f in Cp_3Ce; 55% 5f in Cp_3Dy). Also like the actinides, this dramatic increase does not lead to a significant increase in metal–ligand interaction, as measured by the 4fϕ–4fϕ splitting (Table II). However, $\Delta E_{f\phi}$ for the lanthanide compounds is significantly less than for the actinide compounds. Taking this measurement to be representative of the bonding ability of the f orbitals, it appears that the magnitude of the interaction of the lanthanide 4f orbitals with the ligands is only 60–70% of the actinide 5f-orbital interaction.

The differences in bonding capability of the 4f orbitals vs the 5f orbitals can be explained by comparing the radial extension and energies of these orbitals. Figure 4 includes contour diagrams of the $4f_{z^3}$ orbitals of Cp_3Pr and Cp_3Dy. As was the case with the 5f orbitals of the actinide elements, the 4f orbitals of the lanthanide elements contract across the series. Comparison of the 4f orbitals with the 5f orbitals reveals that the radial extension of the $4f_{x^3}$ orbital of Cp_3Pr is essentially identical with the radial extension of the $5f_{z^3}$ orbital of Cp_3Cf. The differences between the 4f orbitals and the 5f orbitals are clear when we realize that praseodymium is the second lanthanide metal while californium is the ninth actinide metal. As such, the 4f-orbital energy of Cp_3Pr is >1.0 eV higher in energy than the 5f-orbital energy of Cp_3Cf. Taking the energy of the f orbitals into consideration, a truer comparison would involve the 4f orbitals of Cp_3Dy with the 5f orbitals of Cp_3Cf. The difference in the radial extension of these orbitals is much more pronounced and accounts for the weaker bonding ability of the 4f orbitals relative to the 5f orbitals.

The $1a_2''$ and 1e′ orbitals, which have a negligible effect on the bonding in the actinide compounds, have a slight influence on the bonding in Cp_3Ln compounds. This slight influence for both orbitals is actually an antibonding interaction resulting from the filled "semicore" 5p orbitals of the lanthanide metal. This effect is more pronounced for the lanthanide metals than for the actinide metals; this is due to the higher energy of the 5p orbitals, ranging approximately from −20 eV in Cp_3Ce to −23 eV in Cp_3Dy, as compared to the energy of the 6p orbitals, ranging from −23 eV in Cp_3U to −24 eV in Cp_3Cf. Although these differences exist, these orbitals are not the primary source of the bonding interactions in these compounds and should not be considered as significantly important.

In contrast to the actinide compounds, the π_1-based $1a_1$ orbital has no influence on the bonding in the Cp_3Ln compounds. This difference is primarily due to the higher energy of the 6s orbital of the lanthanide metals relative to that of the 7s orbital of the actinide metals. Support for this conclusion comes from the amount of s admixture in the s/d_{z^2} hybrid orbital. This ranges from 4% to 7% for the lanthanide metals compared with 11% to 14% for the actinide metals, indicating that the 6s orbital has a greater energy separation from the 5d orbitals in the lanthanides than the 7s orbital has from the 6d orbitals in the actinides. This is consistent with experimental results on the free ions.[30]

Comparison with a Transition-Metal Analogue. Only one transition-metal, zirconium, has been shown unequivocally to adopt a geometry in which three Cp ligands are all bound to the metal in an η^5 fashion. Each of the three compounds that are known to have this coordination geometry, $(\eta^5\text{-}C_5H_5)_3Zr(\eta^1\text{-}C_5H_5)$,[40] $Cp_3ZrH(AlEt_3)$,[41] and Cp_3ZrCl,[42] has an average Zr–C(η^5-Cp) distance of 2.58 Å. However, these compounds contain a fourth ligand, which causes the three Cp ligands to pyramidalize, destroying the pseudo-D_{3h} geometry. Also, the metal ion in these compounds is Zr(IV), in contrast to the +3 oxidation state of the actinide and lanthanide ions in the compounds discussed thus far. In order to keep all the arguments consistent and to continue to make use of the high symmetry that describes the actinide and lanthanide bonding so well, we have investigated a hypothetical Zr(III) compound, Cp_3Zr (Zr–C = 2.58 Å),[43] with the same pseudo-D_{3h} geometry found for the actinide compounds.

The obvious major difference between a transition metal and an actinide or lanthanide is the former's lack of valence f orbitals. As a result, the $1a_2'$ orbital of Cp_3Zr remains a high-energy, ligand-localized orbital that is metal–ligand nonbonding. The small stabilization energy of the corresponding ligand orbital, 0.03 eV, lends support to the validity of the calculated energies.

The π_2-based 1e″ and 2e′ orbitals of Cp_3Zr exhibit major differences from those in the Cp_3An compounds. The total Zr participation is 39% in the 1e″ MO and 30% in the 2e′. In the

(39) Like Cp_3U, the 2e′ and 1e″ orbitals are nearly isoenergetic in Cp_3Ce, resulting in mixing of these orbitals, which both transform as e representations under the lower C_{3v} symmetry of the calculations. Therefore, the value for Cp_3Pr is given here. In no way does this affect the arguments.

(40) (a) Rogers, R. D.; Vann Bynum, R.; Atwood, J. L. *J. Am. Chem. Soc.* **1978**, *100*, 5238–5239. (b) Kulishov, V. I.; Brainina, E. M.; Bokiy, N. G.; Struchkov, Yu. T. *J. Chem. Soc. D* **1970**, 475.

(41) Kopf, J.; Vollmer, H.-J.; Kaminsky, W. *Cryst. Struct. Commun.* **1980**, *9*, 985–990.

(42) Strittmatter, R. J.; Rhodes, L. F.; Morris, D. E.; Rogers, R. D.; Bursten, B. E.; Sattelberger, A. P., manuscript in preparation.

(43) Whereas the Zr–C bond distance is expected to be longer in a Zr(III) compound than in a Zr(IV) compound, the 2.58-Å bond distance found for these compounds is already quite long compared to a "typical" Zr(IV)–C(Cp) bond.[43a] Therefore, this distance was not lengthened further: Cardin, D. J.; Lappert, M. F.; Raston, C. L. *Chemistry of Organo-Zirconium and -Hafnium Compounds*; Wiley: New York, 1986.

1e″ orbital, the metal contribution is entirely from the 4dπ orbitals, and that in the 2e′ MO is 2% pπ and 28% 4dδ. This is in stark contrast to the actinide orbitals, in which the metal participation ranges from 20% to 13% 6dπ in the 1e″ orbital, and from 16% to 12% 6dδ in the 2e′. While it is true that the 1e″ orbital of the later actinides contains significant contributions from the 5fδ orbitals, it was shown that these orbitals are not as proficient in bonding the ligands as are the 6dπ orbitals. These major differences are demonstrated most clearly in the stabilization energies of the corresponding ligand orbitals (Table III). Upon interaction with the zirconium atom, the ligand-based e″ orbital is stabilized by 0.24 eV more than upon interaction with the uranium atom. This zirconium–actinide stabilization difference increases to 0.48 eV when the actinide metal is californium. The 2e′ orbital, which is the orbital responsible for the primary bonding interaction, also displays a sizable zirconium–actinide stabilization difference of at least 0.48 eV (favoring Zr) regardless of actinide metal.

The $1a_2''$ and the π_1-based 1e′ orbitals of Cp_3Zr show no antibonding influences that are due to the core 4p orbitals of zirconium. This is not surprising; unlike the semicore nature of the np orbitals of actinides and lanthanides, the np orbitals of a transition metal are truly core orbitals and generally have no influence on the bonding. The energy of the zirconium 4p orbitals in Cp_3Zr is −31 eV, at least 7 eV lower than the 6p orbitals of any of the actinides. The 1e′ orbital actually has a slight bonding contribution, as exhibited by the 0.15 eV stabilization of the ligand orbital.

The π_1-based $1a_1'$ orbital of Cp_3Zr is similar to the analogous orbital of the actinide compounds. The zirconium participation in this orbital is 11% 5s and 2% 4dσ and the stabilization energy is <0.1 eV less than that found for the actinide complexes. This is in contrast to the lanthanide complexes, which have a stabilization difference of >0.3 eV in this orbital when compared with the actinide compounds.

Conclusions

Cp_3An compounds, where An = U through Cf, have been investigated via Xα–SW molecular orbital calculations with quasi-relativistic corrections. The 5f-orbital energy of the metals drops >1.2 eV across the series while the 6d-orbital energy rises. Consistent with these trends, the metal 5f-orbital participation in the M–Cp bonding orbitals increases dramatically to the right of the series, and the metal 6d-orbital participation decreases. Although this results in an increase in the total metal participation as we proceed to the right in the series, the greater metal participation in the bonding orbitals does not necessarily imply a greater metal–ligand interaction to the right of the series.

The metal–ligand bonding reflects the high symmetry of the pseudo-D_{3h} structure of the compounds, rendering a detailed analysis of individual orbitals very instructive. This analysis reveals that the 6d orbitals of the actinide metals are more important in bonding the ligands than are the 5f orbitals and, more specifically, that the 6dδ set of orbitals is most important. The greater radial extension of the 6d orbitals vs the 5f orbitals is responsible for this effect. One orbital is restricted by symmetry to interact solely with a metal f orbital. Although this interaction is relatively strong, it does not increase across the series despite a more favorable energy match of the 5f orbitals of the later actinides with the ligand orbital. This is due to a contraction of the 5f orbitals across the series. A minor bonding interaction occurs involving the 7s orbital of the metal. In addition, the semicore 6p orbitals of the actinides show a very slight antibonding influence on the ligands.

A comparison of the actinide results to results on analogous Cp_3Ln compounds reveals some minor differences. The orbital energies of the 4f and 5d orbitals of the early lanthanide metals resemble the 5f- and 6d-orbital energies of the middle actinide metals while the orbital energies of the late lanthanides are similar to those of the late actinides. This is consistent with the "lanthanide-like" behavior of later actinide elements.[44] The 5d orbitals of the lanthanides and the 6d orbitals of the actinides have approximately equal capability to bond to the Cp ligands. However, the 4f orbitals of the lanthanides do not interact with the ligands to the same extent as the 5f orbitals of the actinides. This can be attributed to the differences in radial extension and energies of the two sets of orbitals. Due to its relatively higher energy, the 6s orbital of the lanthanide metals is not involved in any bonding interaction. Although still extremely small, the antibonding influence on the ligands by the semicore 5p orbitals of the lanthanides is greater than that of their actinide analogues.

The obvious difference between a transition-metal compound and the actinide compounds is the lack of valence f orbitals for the transition-metal compound. Calculations on Cp_3Zr indicate that the 4d orbitals of zirconium interact with the ligands to a much greater extent than do the 6d orbitals of the actinides. In spite of its not possessing f orbitals, the interaction of the Zr atom with the Cp ligands is significantly greater than that in actinide or lanthanide complexes.

In summary, these calculations provide support for the conclusions that have been drawn previously concerning the covalency of metal–cyclopentadienyl interactions. Cp_3An compounds of the early actinides appear to be more covalent than those of the later actinides and the lanthanides. Additional differences exist between the Cp_3An compounds and the Cp_3Ln compounds, but most of these occur in orbitals that are not primarily responsible for the bonding of ligands. Major differences in the primary bonding orbitals exist between the Cp_3An compounds and Cp_3Zr, with the overall bonding considerably greater in the latter.

Computational Details

All of the calculations reported here employ the SCF–Xα–SW molecular orbital method[26] and were undertaken with existing codes that incorporate the quasi-relativistic corrections of Wood and Boring.[45] The initial charge densities were generated by a superposition of the neutral atomic charges as given by the method of Herman and Skillman.[46] The α exchange parameters were those of Schwarz,[47] and a valence-electron weighted average was used for the intersphere and outer-sphere regions. Overlapping atomic sphere radii were determined by the nonempirical procedure of Norman, using 89% of the atomic number radii.[48] Partial wave basis sets consisting of spherical harmonics through $l = 4$ on the outer sphere, $l = 3$ on the actinides and lanthanides, $l = 2$ on zirconium, $l = 1$ on carbon, and $l = 0$ on hydrogen were used. The molecular calculations were converged with ground electron configurations corresponding to the $5f^n6d^0$ configuration for the actinides and the $4f^n5d^0$ configuration for the lanthanides (n is the number of metal-based electrons in the +3 oxidation state; see ref 17b). A $4d^1$ ground electron configuration was used for zirconium(III).

The calculations were performed under C_{3v} symmetry. The M–C distances were chosen by comparison to known structures, as discussed in the text. The C–C distances were 1.39 Å and the C–H distances were 1.08 Å. The Cp(centroid)–M–Cp(centroid) angle was 120°.

The fragment analysis was carried out by truncating the potential of the converged molecule such that it contained contributions only from those atoms present in the fragment of interest. This was then used as input for one iteration with use of mixing 0.2% of the new potential into the old. In this manner, the energies of the one-electron orbitals in the molecular fragment were determined in the potential of the converged molecule.[33]

The charge density levels were partitioned into those from each symmetry-adapted basis function rather than by spherical harmonic angular quantum numbers. The intersphere and outer-sphere charges were included in this partitioning. This approach, which has been described previously,[49] gives a more extensive breakdown of the charge density, facilitating a pseudo-LCAO interpretation of the orbitals.

Acknowledgment. We gratefully acknowledge support for this research from the Division of Chemical Sciences, Office of Basic Energy Sciences, U.S. Department of Energy (Grant DE-

(44) Cotton, F. A.; Wilkinson, G. *Advanced Inorganic Chemistry*, 5th ed.; Wiley: New York, 1988; Chapter 21.

(45) Wood, J. H.; Boring, A. M. *Phys. Rev. B* **1978**, *18*, 2701–2711.

(46) Herman, F.; Skillman, S. *Atomic Structure Calculations*; Prentice-Hall: Englewood Cliffs, NJ, 1963.

(47) (a) Schwarz, K. *Phys. Rev. B* **1972**, *5*, 2466–2468. (b) Schwarz, K. *Theor. Chim. Acta* **1974**, *34*, 225–231.

(48) Norman, J. G. *J. Chem. Phys.* **1974**, *61*, 4630.

(49) Bursten, B. E.; Schneider, W. F. *Inorg. Chem.* **1989**, *28*, 3292–3296.

FG02-86ER13529). We also acknowledge Mr. William F. Schneider for modifications to the Xα-SW program and Dr. Melanie Pepper for helpful discussions. R.J.S. acknowledges Amoco for an Industrial Fellowship (1988) and The Ohio State University for a Presidential Fellowship (1989-1990).

Supplementary Material Available: Table IV, which contains the energy, electron occupancy, total metal participation, and relative participation of individual metal atomic orbitals for all valence orbitals discussed for each compound (9 pages). Ordering information is given on any current masthead page.

Insertion of Rhodium into the Carbon-Sulfur Bond of Thiophene. Mechanism of a Model for the Hydrodesulfurization Reaction

William D. Jones* and Lingzhen Dong

Contribution from the Department of Chemistry, University of Rochester, Rochester, New York 14627. *Received June 4, 1990*

Abstract: The reaction of $(C_5Me_5)Rh(PMe_3)(Ph)H$ with thiophene leads to the elimination of benzene and oxidative addition of the thiophene C-S bond across the Rh(I) center, giving $(C_5Me_5)Rh(PMe_3)(SCH{=}CHCH{=}CH)$. Similar reactions occur with 2-methylthiophene, 3-methylthiophene, 2,5-dimethylthiophene, benzothiophene, and dibenzothiophene. Selectivity studies performed with these complexes are consistent with the coordination of sulfur to rhodium prior to C-S bond cleavage. Reversible reductive elimination of thiophene occurs at ~80 °C. The diene portion of the C-S insertion ligand undergoes a Diels-Alder reaction with dimethyl acetylenedicarboxylate to give dimethyl phthalate as a major product. The dimethylthiophene complex $(C_5Me_5)Rh(PMe_3)(SCMe{=}CHCH{=}CMe)$ was structurally characterized, crystallizing in the monoclinic space group $P\bar{1}$ with a = 8.707 (8) Å, b = 14.157 (15) Å, c = 8.637 (5) Å, α = 100.90 (8)°, β = 106.07 (6)°, γ = 87.85 (8)°, V = 1004 (3) Å^3, and Z = 2.

Introduction

Homogeneous modeling of the heterogeneous hydrodesulfurization (HDS) process[1] has focused upon reactions of metal complexes with thiophene and thiophene derivatives in an effort to elucidate the most important mechanistic pathways. Two general varieties of mechanisms have been proposed, one involving initial π coordination of the thiophene either through one double bond[2] or through the entire π system,[3] and the other invoking insertion of the metal into the carbon-sulfur bond through an S-bound complex.[4] While most of the homogeneous studies have pointed toward η^4- or η^5-thiophene intermediates,[5-11] evidence has also appeared for S-bound thiophene[12-19] and for metal insertion into the C-S bond.[20] We report here the evidence for insertion of a metal into the carbon-sulfur bond of thiophene by way of initial coordination through sulfur.

Results

Reactions with Thiophene Derivatives. The complex $(C_5Me_5)Rh(PMe_3)(Ph)H$ (**1**) has been shown to behave as a thermal precursor for the generation of the unsaturated fragment $[(C_5Me_5)Rh(PMe_3)]$, which is active toward the oxidative addition of a variety of carbon-hydrogen bonds.[21] Recently, isolation of η^2-arene complexes was found to be possible with fused polycyclic aromatics.[22] In examining similar reactions with heterocyclic aromatics, we discovered that thiophene reacts with **1** at 60 °C in hexane solution to give benzene plus a single organometallic product in high yield in which all four of the thiophene hydrogens display distinct resonances in the ^{1}H NMR spectrum (Table I). Furthermore, the ^{31}P NMR spectrum shows a low-field doublet with J_{Rh-P} = 160 Hz, indicative of a Rh(III) complex. The absence of a hydride resonance in the ^{1}H NMR spectrum rules out a C-H bond oxidative addition adduct. The presence of a doublet of doublets in the ^{13}C NMR spectrum provides strong evidence for the formulation of the product as the C-S insertion adduct, $(C_5Me_5)Rh(PMe_3)(SCH{=}CHCH{=}CH)$ (**2**) (eq 1).

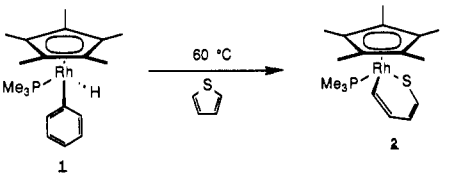

1 2 (1)

A similar reaction of **1** with 2,5-dimethylthiophene led to the formation of the analogous insertion product, $(C_5Me_5)Rh$-

(1) Schuman, S. C.; Shalit, H. *Catal. Rev.* **1970**, *4*, 245-313.
(2) Kwart, H.; Schuit, G. C. A.; Gates, B. C. *J. Catal.* **1980**, *61*, 128-134.
(3) Schoofs, G. R.; Preston, R. E.; Benziger, J. B. *Langmuir* **1985**, *1*, 313-320.
(4) Kolboe, S. *Can. J. Chem.* **1969**, *47*, 352-355.
(5) Lockemeyer, J. R.; Rauchfuss, T. B.; Rheingold, A. L.; Wilson, S. R. *J. Am. Chem. Soc.* **1989**, *111*, 8828-8834.
(6) Lesch, D. A.; Richardson, J. W.; Jacobson, R. A.; Angelici, R. J. *J. Am. Chem. Soc.* **1984**, *106*, 2901-2906.
(7) Hachgenei, J. W.; Angelici, R. J. *Organometallics* **1989**, *8*, 14-17.
(8) Spies, G. H.; Angelici, R. J. *Organometallics* **1987**, *6*, 1897-1903.
(9) Hachgenei, J. W.; Angelici, R. J. *J. Organomet. Chem.* **1988**, *355*, 359-378.
(10) Chen, J.; Angelici, R. J. *Organometallics* **1989**, *8*, 2277-2279.
(11) Ogilvy, A. E.; Skaugset, A. E.; Rauchfuss, T. B. *Organometallics* **1989**, *8*, 2739-2741.
(12) Choi, M.-G.; Angelici, R. J. *J. Am. Chem. Soc.* **1989**, *111*, 8753-8754.
(13) Draganjac, M.; Ruffing, C. J.; Rauchfuss, T. B. *Organometallics* **1985**, *4*, 1909-1911.
(14) Kuehn, C. G.; Taube, H. *J. Am. Chem. Soc.* **1976**, *98*, 689-702.
(15) Wasserman, J. J.; Kubas, G. J.; Ryan, R. R. *J. Am. Chem. Soc.* **1986**, *108*, 2294-2301.
(16) Goodrich, J. D.; Nickias, P. N.; Selegue, J. P. *Inorg. Chem.* **1987**, *26*, 3424-3426.
(17) Kuhn, N.; Schumann, H. *J. Organomet. Chem.* **1984**, *276*, 55-66.
(18) Catheline, D.; Astruc, D. *J. Organomet. Chem.* **1984**, *272*, 417-426.
(19) Guerchais, V.; Astruc, D. *J. Organomet. Chem.* **1986**, *316*, 335-341.
(20) Chen, J.; Daniels, L. M.; Angelici, R. J. *J. Am. Chem. Soc.* **1990**, *112*, 199-204.
(21) Jones, W. D.; Feher, F. J. *Acc. Chem. Res.* **1989**, *22*, 91-100.
(22) Jones, W. D.; Dong, L. *J. Am. Chem. Soc.* **1989**, *111*, 8722-8723.

0002-7863/91/1513-559$02.50/0